

# Development, Characterization and Short-Term Stability Studies of Chitosan-Lipid Hybrid Nanocarrier System

Manoj B. Shinde<sup>1,2\*</sup>, Adhikrao V. Yadav<sup>2</sup>

<sup>1</sup>Department of Pharmaceutics, Satara College of Pharmacy, Satara, Maharashtra, India.

<sup>2</sup>Department of Pharmaceutics, Government College of Pharmacy, Karad, Maharashtra, India.

Received: 18<sup>th</sup> October, 2022; Revised: 13<sup>th</sup> January, 2023; Accepted: 15<sup>th</sup> March, 2023; Available Online: 25<sup>th</sup> June, 2023

## ABSTRACT

Pharmaceutical nanocarriers have recently been widely used to improve drug performance and reduce side effects. They have been shown to be effective for controlled release, sustained release, and targeted delivery. It is also possible to accomplish effective drug utilization, improve permeability, and attain selectivity of drugs. Chitosan polymer attracted the attention of formulation scientists due to its biocompatible, biodegradable nature and utility in drug delivery as a permeation enhancer, as well as its ability to achieve sustained, controlled, site-specific release. Furthermore, it has been shown to be an efficacious counter to both gram -ve and +ve bacteria. Chitosan is a useful carrier for a variety of nanosystems. Targeting the intestinal region of the gastrointestinal track the lymphatic system and other novel approaches will be possible if combined with long-chain fatty lipids. The present work developed a chitosan-lipid nanocarrier system (CLNS) by melt emulsification with sonication. The prepared system was assessed for size analysis, and determination of PDI, zeta potential and the findings were  $221.3 \pm 3.2$  nm,  $0.251 \pm 0.01$ ,  $26.9 \pm 2.2$  mV, respectively. FTIR analysis reveals the polymer's compatibility with lipid. DSC and XRD analysis confirmed the presence of amorphous CLNS. The TEM findings suggest that CLNS have a nearly spherical shape with a smooth surface morphology. Furthermore, the carrier system was tested for short-term stability studies, and it was observed that the system is more stable at refrigerated ( $4^{\circ}\text{C}$ ) and normal environmental conditions ( $25 \pm 2^{\circ}\text{C} / 60 \pm 5\%$  RH) than that of the accelerated conditions ( $40 \pm 2^{\circ}\text{C} / 75 \pm 5\%$  RH).

**Keywords:** Chitosan, Lipid, Nanocarriers, Sonication, Stability studies.

International Journal of Drug Delivery Technology (2023); DOI: 10.25258/ijddt.13.2.16

**How to cite this article:** Shinde MB, Yadav AV. Development, Characterization and Short-Term Stability Studies of Chitosan-Lipid Hybrid Nanocarrier System. International Journal of Drug Delivery Technology. 2023;13(2):562-567.

**Source of support:** Nil.

**Conflict of interest:** None

## INTRODUCTION

Nanotechnology has become very popular in the pharmaceutical field because of its tremendous benefits in improving the efficacy and proper utilization of drugs. Many nanosystems act as carriers, so it helps formulators reach their drug delivery goals. Nanocarriers overcome the drawbacks of conventional preparations. Nanoparticles, nanoemulsions, nanospheres, nanocapsules and vesicular nanocarriers, such as niosomes and liposomes, are all included under the umbrella term "nanocarriers."<sup>1</sup> Research focuses on developing an advanced nanotechnological approach as a selective carrier system for the drug delivery to the target site. Eventually, tiny nanocarriers along the very greater numbers could be inaccessible sites, primary tumor cells and inflamed tissues. For the selective delivery of drug substances, better permeability, a retention effect, and a changed lymphatic drain may all be advantageous.<sup>2</sup> Many times, these carriers

could deliver therapeutics to a specific site which helps improve solubility, extend the duration of action, and protect against various enzymatic degraders while also increasing bioavailability to achieve optimum therapeutic effectiveness.<sup>3</sup> Lipid nanoparticles, metal nanoparticles, liposomes, and polymer-based nanoparticles are the most popular nanocarriers utilized in systems to deliver drugs.<sup>4</sup> However, there are some restrictions on each of these nanocarriers. For example, some of these are primarily used for lipophilic medications. During storage, solid lipid nanoparticles are physically unstable. The polymeric nanoparticles may suddenly release hydrophilic drug entities. They become stable during storage, but specified conditions will be needed for their possible antigenicity and degradation. Liposomes have low drug embedment efficiency and leakage of hydrophilic medicaments.

Polymeric nanocarriers have a number of advantageous qualities, such as biocompatibility, biodegradability, the ability to modify the surface, and simplicity of functionalization.

\*Author for Correspondence: manojshinde2489@gmail.com

The high surface-volume ratio contributes significantly to the stability of polymeric nanocarriers.<sup>5</sup> Chitosan is a well-known naturally occurring biocompatible, safe, and degradable material that offers additional advantages like mucoadhesive potential and enhanced cell permeation properties. Chitosan-based delivery systems have a lot of benefits for different routes, including the preferred ocular, nasal, and oral mucosa.<sup>6</sup> It is possible to fabricate chitosan nanosystems using simple and tolerant procedures. Because of this, chitosan nanoparticles can be used to make a wide range of medicines and have been shown to work well as adjuvants in vaccines.<sup>7</sup> Lipid nanocarriers are ideally suited for transporting lipid-soluble drugs.<sup>8</sup> In addition, lipid systems administered orally show adherence with surface of gut region, increasing the time of residence and improving absorption.<sup>9</sup> Furthermore, lipidic nanosystems may protect loaded actives from enzymatic and chemical deterioration while being gradually released at particular site from carrier matrix of lipid. Consequently, the advantageous biocompatibility and physiological characteristics of a particular type of lipid may alleviate various adverse effects. Moreover, micellar solubility and permeability of drugs through intracellular, paracellular, and uptake by patches of Peyer's can play a crucial character in enhancing bioavailability after oral administration.<sup>10</sup> In particular, lipidic nanocarriers have great potential for enhancing the solubility of different lipid drugs through aquatic unstirred layers via various strategic approaches.<sup>11</sup> However, lipid-based carriers have some limitations, like less entrapment and drug expulsion while storage.<sup>12</sup>

Despite the limitations of pure individual nanocarriers, an approach with combinational carriers may be helpful in conquering them. Polymer–lipid hybrid nanoparticles are one of the recommended nanocarriers for the delivery of both hydrophilic and lipophilic drugs.<sup>13</sup> With this system, it is possible to overcome the limitations of polymeric and lipid nanocarriers and take advantage of both. In the present study, a chitosan-based polymer lipid nanocarrier system was developed so that they could act as a matrix and be useful for sustained release, enhancing bioavailability, increasing the entrapment efficiency of drugs, and targeting the intestinal portion of the GIT. Targeting conditions such as cancers and infections will also be possible by selectively introducing formulations into the lymphatic system and macrophages. The basic objective of entitled research was the development of stable as well as ideal nanocarrier system.

## MATERIALS AND METHODS

### Materials

Polymer chitosan (deacetylation degree more than 90%) was purchased from SRL Laboratories Pvt. Ltd., Mumbai, India., lipid glycerol monostearate was procured from Loba cheme in India, Poloxamer 188 purchased from Yarrow Chemicals, India. Tween 80 procured from Bangalore Fine Chem, all solutions, reagents, and chemicals used were as per analytical standards.

## Methods

### *Preparation of chitosan lipid hybrid nanocarrier system*

CLNS were formulated through melt emulsification and probe sonication. The chitosan solution was prepared by stirring at 700 rpm for 12 hours in a 1% acetic acid solution. By mixing both surfactants, tween 80 and poloxamer 188 (ratio of 2:1) with distilled water, a 1.5% surfactant solution was prepared. With continuous stirring, the chitosan solution and surfactant solution were thoroughly combined. The temperature of the aqueous phase was set to 70°C. Simultaneously, glycerol monostearate was melted at 70°C. The lipid kept at required temperature was then added into aqueous portion, which was kept at the same temperature and stirred with 2000 rpm for one hour. Stirring was continued until the dispersion temperature reached normal and sonicated for 15 minutes with a probe sonicator (Hielscher, ultrasound UP-50 H, Germany) to make nanoscale CLNS.

### *Characterization of PLNs*

DLS technique was chosen to measure particulate size, PDI, and well zeta potential of CLNS (HORIBA SZ-100 Ver. 2.40, Japan). FTIR study was conducted to analyse functionality for individual components and final formulation. FTIR spectrophotometer (Bruker Alpha 100508, India) was used to record polymer and lipid infrared spectrum in the 4000 to 400  $\text{cm}^{-1}$  wavelength region. DSC studies (TA Instruments, USA, SDT Q600 V20.9 Build 20) were conducted to analyze thermal characteristics of nanocarriers. The XRD analysis was conducted with an advanced Bruker AXS D8 diffractometer and Diffrac plus V1.01 software. For confirmation of shape and size of CLNS the, transmission electron microscopy (JEOL-JEM 2100 +, Japan) was used.

### *Short-term stability studies*

The stability studies of CLNS has been evaluated as per guidelines from the ICH. In the environmental test chamber, 10 mL of optimized CLNS were placed in three separate glass containers and they were stored to refrigeration conditions ( $4 \pm 2^\circ\text{C}$ ), normal or common conditions ( $25 \pm 2^\circ\text{C}/60 \pm 5\%$  RH) and accelerated or elevated conditions ( $40 \pm 2^\circ\text{C}/75 \pm 5\%$  RH) in stability chamber (REMI Electrotechnik Ltd., Mumbai). The samples of specified conditions were evaluated for particle size analysis, PDI determination and zeta potential studies at predetermined intervals of time for 0, 1, 3, and 6 months. The findings of the studies were statistically compared.<sup>8,14,15</sup>

## RESULTS AND DISCUSSION

### Characterization of Prepared Nanocarrier System

#### *Particle size, dispersity and surface charge of CLNS*

Figure 1 depicts the dispersion's particle size, its dispersity and surface charge (zeta potential) as per DLS studies. Results from three iterations were averaged to determine the values. It was revealed that the particulate size, PDI & zeta potential for dispersion were correspondingly  $221.3 \pm 3.2$  nm,  $0.251 \pm 0.01$  &  $26.9 \pm 2.2$  mV. The found particle size was promising and

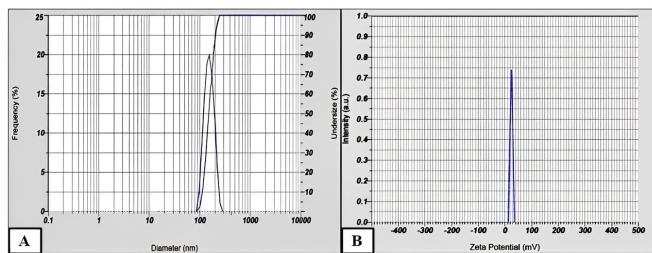


**Figure 1:** DLS results for A. Particle size with distribution and B. Zeta potential for chitosan lipid nanocarrier system

will be useful to accomplish desired goals, such as targeting a specific site. The sample's PDI was  $< 0.3$ , demonstrating that particle size distribution was desirable. The value of zeta potential was positive, possibly due to positive groups of chitosan at the surface. The zeta potential was also appropriate so that particle aggregation will be at a minimum and stability will increase.

#### Analysis with FTIR Spectroscopy

Figure 2 represents FTIR spectra for polymer chitosan, lipid GMS and CLNS. The principal absorption band for the chitosan polymer may be related to OH stretch at wavenumber  $\lambda = 3419.77 \text{ cm}^{-1}$ .<sup>16</sup> Bands of CH stretching and C=O stretching of secondary amide are shown at wavenumber  $\lambda = 2848.11$  &  $1731.21 \text{ cm}^{-1}$ , correspondingly.<sup>17</sup> Wavenumber  $1581.32$  represents the bending vibrations for N-H. Accountability of NH stretching for ether and amide bonds, also the NH stretching of tertiary amide band, might be for the peaks at  $\lambda = 1421.32$  &  $1372.32 \text{ cm}^{-1}$ , respectively. A peak at wavenumber  $1708.30$  is for the R-NH<sub>2</sub> group.<sup>18</sup> Primary and secondary hydroxyl groups are related to peaks shown at wavenumber  $\lambda = 1038.55$  &  $1149.32 \text{ cm}^{-1}$  correspondingly.<sup>19</sup> For GMS lipid, the C-O and C=O ester groups are associated with stretching vibration at wavenumber  $1113.79$  and  $1639.23 \text{ cm}^{-1}$ , correspondingly. The peaks at wavenumber  $2846.83$  and  $2914.25$  indicate bands with methylene induced due to symmetric and asymmetric stretching vibrations, respectively.<sup>20</sup> A stretching vibration for hydroxyl group is at an absorption band of  $3391.49 \text{ cm}^{-1}$ .<sup>21</sup> The vibration (rocking) for (CH<sub>2</sub>)<sub>n</sub> ( $n \geq 4$ ) groups and the vibration (deformation) of CH<sub>3</sub> or CH<sub>2</sub> groups, are responsible for absorption maxima at  $1464.32$  and  $796.10 \text{ cm}^{-1}$  correspondingly. The OH stretching vibrations at a wavelength  $3392.40$  in CLNS, caused by weak bonding hydrogen, overlap when spectras of CLNS and polymer chitosan are compared. Bending vibrations for N-H<sub>2</sub> decreased from  $1581.32$  to  $1463.05 \text{ cm}^{-1}$  as a result of hydrogen bonding. The increased methylene bending vibrations in CLNS from  $2914.25$  to  $2914.83 \text{ cm}^{-1}$  and from  $2846.83$  to  $2847.67 \text{ cm}^{-1}$  due to the electrostatic interaction, according to a spectral comparison between CLNS and GMS lipid. The CLNS structure also showed additional lipid peaks. The FTIR spectra of nanoparticles showed essentially unchanged peaks but with less intensity due to a partial loss of crystallinity in the nanoparticles. The CLNS spectra preserved all the characteristics of the corresponding polymer and lipid components.<sup>22</sup> It is likely

that no new chemical bonds between these functional groups in the polymer and the lipid were formed after the formulation of the nanoparticles because there were no noticeable changes in the absorption bands of the nanoparticles.

#### DSC analysis of CLNS

Figure 3 displays the DSC thermograms for the chitosan polymer, lipid GMS, and CLNS. As shown in Figure, the evaporation of absorbed water causes the chitosan to typically exhibited a sharp endothermic peak at  $63.70^\circ\text{C}$ . With this an exothermic baseline deviation that started at around  $270.21^\circ\text{C}$  indicated the beginning of chitosan degradation. These results are as per earlier studies.<sup>23</sup> For GMS lipid the endothermic peak showed a melting point of around  $64.32^\circ\text{C}$ .<sup>24</sup> As observed in Figure, at  $180.50^\circ\text{C}$  a new endothermic elevation has been shown in the CLNS DSC curve, which is situated between the endothermic peaks of chitosan ( $270.21^\circ\text{C}$ ) and GMS ( $64.32^\circ\text{C}$ ), indicating the hybridization of polymer and lipid.

#### XRD studies of CLNS

Figure 4 demonstrates the GMS, CLNS, and chitosan XRD patterns. The significant peaks ( $2\theta$ ) at  $10.80$  and  $19.97^\circ$  for the chitosan polymer demonstrated the high degree of crystallinity of the compound.<sup>25</sup> While peaks indicate the crystallinity of GMS at  $18.85$  and  $22.58^\circ$  in its X-ray diffraction patterns.<sup>26</sup> The crystallinity of CLNS revealed characteristic  $2\theta$  at the polymer-lipid crystallinity point indicating the presence of polymer and lipid peaks that were less intense and less pointed, indicating that the polymer had become amorphized and had been engulfed by lipid to form a matrix. XRD revealed highly disorganized chain alignment following the formation of the nanocarrier matrix.

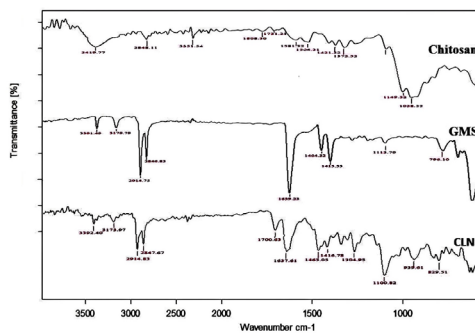


**Figure 2:** FTIR Spectra of chitosan, lipid and CLNS

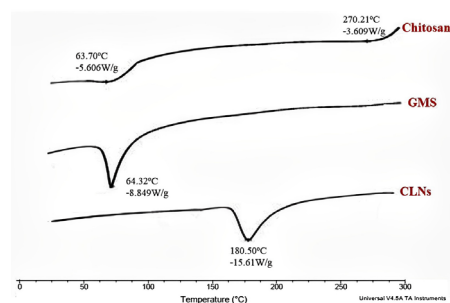


**Figure 3:** DSC thermograms of chitosan, GMS and CLNS

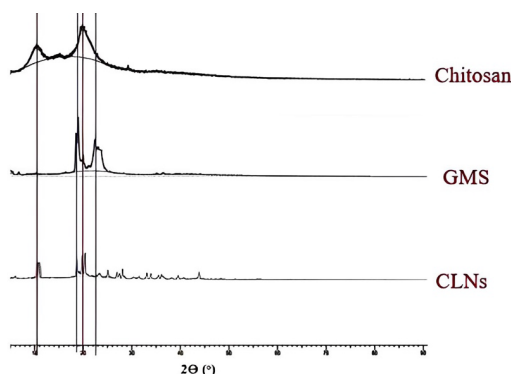


Figure 4: XRD analysis of chitosan, GMS and CLNS

#### Transmission electron microscopy (TEM) Analysis of CLNS

TEM micrographs of prepared CLNS (Figure 5) revealed that the developed nanocarriers are nearly spherical and intact. The particle dimensions measured by TEM were within a range found in DLS (Figure 1). The results reveal that spherical-shaped particles were formulated in dispersion.<sup>27</sup> Additionally, the diameters of CLNS were found to be between 150 to 250 nm. In addition, it indicated that the surface of CLNS is protected by surfactants.<sup>28</sup>

#### Short-term stability studies of CLNS

Table 1, represent the results for short-term stability studies for nanocarriers. Initial particulate size, PDI & zeta potential become nearly identical for all three conditions. In terms of particle size, CLNS preserved under refrigeration at  $4 \pm 2^\circ\text{C}$  and normal conditions i.e. at  $25 \pm 2^\circ\text{C}/60 \pm 5\% \text{RH}$  remained relatively stable for up to period of six months. When CLNS were stored at elevated conditions of  $40 \pm 2^\circ\text{C}$  temperature and  $75 \pm 5\% \text{RH}$ , the size of particles increased with significance (Figure 6). The PDI of CLNS was nearly constant over a six-months period following storage in both refrigerated and normal conditions. However, it moderately increases under elevated storage conditions (Figure 7). The zeta potential decreases slightly under refrigerated and normal conditions, but the differences are statistically insignificant i.e.  $p > 0.05$ . While zeta potential decreased considerably under elevated storage conditions (Figure 8). When nanoparticles stored at temperatures  $4 \pm 2^\circ\text{C}$  (refrigerated condition) and  $25 \pm 2^\circ\text{C}$  temperature with relative humidity  $60 \pm 5\%$  (normal condition), particle growth was slower. But when conditions were accelerated, i.e. at  $40 \pm 2^\circ\text{C}$  temperature and  $75 \pm 5\% \text{RH}$ , the particle size increased due to aggregation because of increased particle-particle collisions due to the system's higher kinetic energy. Compared to samples stored at refrigeration and normal conditions, nanoparticles stored at elevated conditions exhibited a faster decline in zeta potential, indicating that they were less stable. It has been reported that an increase in energy input causes a change in crystallinity of polymer as well as lipid. This reorientation of crystalline structure can ultimately change the surface charge of particles to change a zeta potential.

The obtained results show that the system revealed excellent stability in relation with particulate size, PDI & zeta

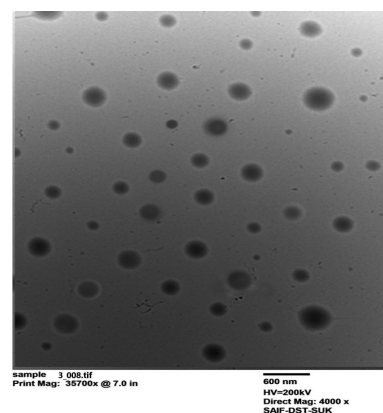


Figure 5: TEM of chitosan lipid nanocarriers

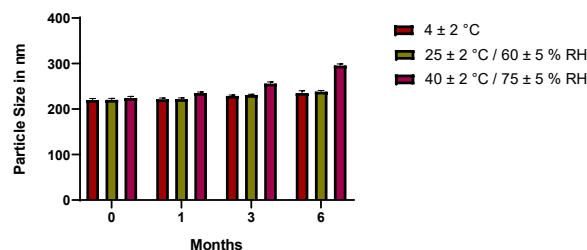


Figure 6: Particle size of CLNS on storage at refrigerated, normal and accelerated conditions

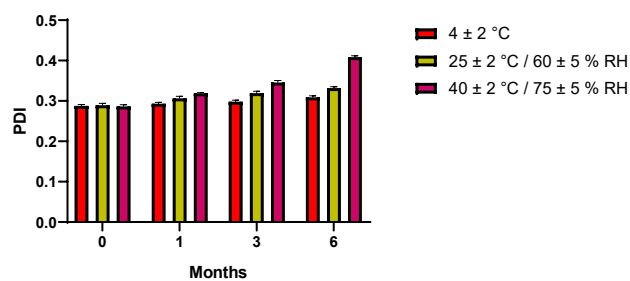
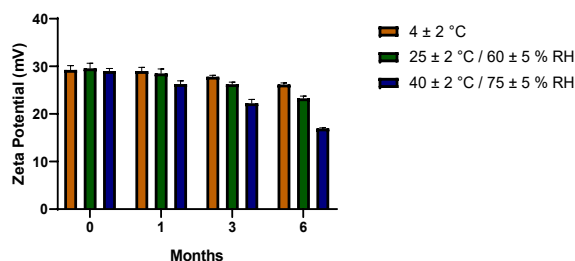


Figure 7: PDI of CLNS on storage at refrigerated, normal and accelerated conditions

potential after a period of 6 months storage at  $4 \pm 2^\circ\text{C}$  and  $25 \pm 2^\circ\text{C}/60 \pm 5\% \text{RH}$ . Higher level of film emulsifier, i.e., presence of surfactant tween 80 and stabiliser poloxamer 188, has been shown to prevent fusion of layered films after collision of particles under refrigeration and normal conditions. The system became less stable on storage at  $40 \pm 2^\circ\text{C}/75 \pm 5\% \text{RH}$ . At high temperature and humidity, particle size, PDI & zeta potential get increased because the dissolution of outer surfactant coating of CLNS, resulting in particle aggregation.<sup>14,29</sup> Data obtained shows that after 6 months of storage, the particle size of all particles retained in nanoscale (Figure 6). Furthermore, for all formulations PDI were less than 0.5, indicating that the CLNS were physically stable in terms of particle size and PDI for 6 months under the mentioned storage conditions (Figure 7). In general, the agglomeration threshold in zeta potential dispersions is less than 15 mV. According to the findings of these studies, zeta potential values were greater than 15, indicating no significant agglomeration of CLNS after 6



**Figure 8:** Zeta potential of CLNS on storage at refrigerated, normal and accelerated conditions

**Table 1:** Particulate size, PDI & zeta potential of CLNS on storage at different conditions

Storage condition		Particle size in nm	Polydispersity index	Zeta potential in mV
Temp & RH	Months			
4 ± 2 °C	0	219.93 ± 3.63	0.287 ± 0.004	29.23 ± 0.83
	1	221.56 ± 2.96	0.293 ± 0.003	29.00 ± 0.90
	3	228.86 ± 2.26	0.298 ± 0.004	27.80 ± 0.30
	6	235.16 ± 5.06	0.309 ± 0.004	26.16 ± 0.34
25 ± 2 °C / 60 ± 5 % RH	0	220.06 ± 3.76	0.289 ± 0.005	29.56 ± 0.24
	1	221.76 ± 2.96	0.306 ± 0.005	28.5 ± 1.00
	3	230.93 ± 1.67	0.319 ± 0.005	26.23 ± 0.47
	6	238.06 ± 2.56	0.331 ± 0.004	23.26 ± 0.54
40 ± 2 °C / 75 ± 5 % RH	0	220.90 ± 3.40	0.286 ± 0.005	29.00 ± 0.60
	1	235.03 ± 2.73	0.319 ± 0.002	26.26 ± 0.76
	3	255.8 ± 4.00	0.345 ± 0.006	22.23 ± 0.93
	6	295.6 ± 3.80	0.408 ± 0.004	16.93 ± 0.17

months of storage (Figure 8). Despite the fact that the properties of CLNS changed at storage conditions  $40 \pm 2^\circ\text{C}/75 \pm 5\% \text{RH}$  in comparison to the normal and refrigerated conditions, the results were within an acceptable range.

## CONCLUSION

This study successfully prepared chitosan-lipid nanocarriers (CLNS) by melt emulsification with sonication method. The prepared nano system showed promising results for particle size of  $221.3 \pm 3.2 \text{ nm}$ , PDI of  $0.251 \pm 0.01$  and the zeta potential of  $26.9 \pm 2.2 \text{ mV}$ . FTIR results suggest that chitosan and GMS was compatible to each other. DSC analysis and XRD study confirmed that the CLNS exist in amorphous form. The TEM findings confirm that CLNS have a nearly spherical shape and smooth surface morphology. From short term stability it was found that CLNS were stable at refrigeration ( $4 \pm 2^\circ\text{C}$ ) and normal storage conditions ( $25 \pm 2^\circ\text{C} / 60 \pm 5\% \text{RH}$ ). Moderate changes have been noticed in particulate size, PDI, and zeta potential of CLNS stored to elevated conditions ( $40 \pm 2^\circ\text{C} / 75 \pm 5\% \text{RH}$ ) for the six months, but observed changes are acceptable. Hence, the prepared nanocarrier system will be used as effective platform to improve drug utilization and selectivity of therapeutic molecules.

## REFERENCES

- Ravichandran R. Nanoparticles in drug delivery: Potential green nanobiomedicine applications. *International Journal of Green Nanotechnology: Biomedicine*. 2009;1(2):B108-B130. Available from: doi.org/ 10.1080/19430850903430427
- Jong WH, Paul JB. Drug delivery and nanoparticles : Applications and hazards. *International Journal of Nanomedicine*. 2008;3(2):133–149.
- Jain AK, Thareja S. In vitro and in vivo characterization of pharmaceutical nanocarriers used for drug delivery. *Artificial Cells, Nanomedicine, and Biotechnology An International Journal*. 2019;47(1):524–539. Available from: doi.org/10.1080/21691401.2018.1561457
- Kumar S, Bhanjana G, Kumar A, Taneja K, Dilbaghi N, Kim KH. Synthesis and optimization of ceftriaxone-loaded solid lipid nanocarriers. *Chemistry and Physics of Lipids*. 2016;200:126–132. Available from: doi.org/10.1016/j.chemphyslip.2016.09.002
- Kowalczyk A, Trzcinska R, Trzebicka B, Müller AHE, Dworak A, Tsvetanov CB. Loading of polymer nanocarriers: Factors, mechanisms and applications. *Progress in Polymer Science journal*. 2014;39(1):43–86. Available from: doi.org/10.1016/j.progpolymsci.2013.10.004
- Tezgel Ö, Szarpak-Jankowska A, Arnould A, Auzély-Velty R, Texier I. Chitosan-lipid nanoparticles (CS-LNPs): Application to siRNA delivery. *Journal of Colloid and Interface Science*. 2018;510:45–56. Available from: doi.org/10.1016/j.jcis.2017.09.045
- Ibrahim HM, El-Bisi MK, Taha GM, El-Alfy EA. Chitosan nanoparticles loaded antibiotics as drug delivery biomaterial. *Journal of Applied Pharmaceutical Science*. 2015;5(10):85–90. Available from: doi.org/10.7324/JAPS.2015.501015
- Youssef A, Dudhipala N, Majumdar S. Ciprofloxacin loaded nanostructured lipid carriers incorporated into in-situ gels to improve management of bacterial endophthalmitis. *Pharmaceutics*. 2020;12(6):572. Available from: doi.org/10.3390/pharmaceutics12060572
- Jaiswal P, Gidwani B, Vyas A. Nanostructured lipid carriers and their current application in targeted drug delivery. *Artificial Cells, Nanomedicine, and Biotechnology*. 2016;44(1):27–40. Available from: doi.org/10.3109/21691401.2014.909822
- Talegaonkar S, Bhattacharyya A. Potential of Lipid Nanoparticles (SLNs and NLCs) in Enhancing Oral Bioavailability of Drugs with Poor Intestinal Permeability. *AAPS PharmSciTech*. 2019;20(3):1-5. Available from: doi.org/10.1208/s12249-019-1337-8
- Nordskog BK, Phan CT, Nutting DF, Tso P. An examination of the factors affecting intestinal lymphatic transport of dietary lipids. *Advanced Drug Delivery Reviews*. 2001;50(1–2):21–44. Available from: doi.org/10.1016/S0169-409X(01)00147-8
- Balguri SP, Adelli GR, Janga KY, Bhagav P, Majumdar S. Ocular disposition of ciprofloxacin from topical, PEGylated nanostructured lipid carriers: Effect of molecular weight and density of poly (ethylene) glycol. *International Journal of Pharmaceutics*. 2017;529(1–2):32–43. Available from: doi.org/10.1016/j.ijpharm.2017.06.042
- Rigi A, Farhadian N, Karimi M, Porozan S. Ceftriaxone sodium loaded onto polymer-lipid hybrid nanoparticles enhances antibacterial effect on gram-negative and gram-positive bacteria : Effects of lipid - polymer ratio on particles size , characterist. *Journal of Drug Delivery Science and Technology*. 2021;63:102457. Available from: doi.org/10.1016/j.

- jddst.2021.102457
14. Yasir M, Chauhan I, Zafar A, Verma M, Noorulla KM, Tura AJ. Buspirone loaded solid lipid nanoparticles for amplification of nose to brain efficacy: Formulation development, optimization by Box-Behnken design, in-vitro characterization and in-vivo biological evaluation. *Journal of Drug Delivery Science and Technology*. 2021;61:102164. Available from: <https://doi.org/10.1016/j.jddst.2020.102164>
  15. Makoni PA, Kasongo KW, Walker RB. Short term stability testing of efavirenz-loaded solid lipid nanoparticle (SLN) and nanostructured lipid carrier (NLC) dispersions. *Pharmaceutics*. 2019;11(8):397. Available from: [doi.org/10.3390/pharmaceutics11080397](https://doi.org/10.3390/pharmaceutics11080397)
  16. Tang ESK, Huang M, Lim LY. Ultrasonication of chitosan and chitosan nanoparticles. *Int J Pharm*. 2003;265(1–2):103–114.
  17. Sankalia MG, Mashru RC, Sankalia JM, Sutariya VB. Reversed chitosan-alginate polyelectrolyte complex for stability improvement of alpha-amylase: Optimization and physicochemical characterization. *European Journal of Pharmaceutics and Biopharmaceutics*. 2007;65(2):215–232. Available from: [doi.org/10.1016/j.ejpb.2006.07.014](https://doi.org/10.1016/j.ejpb.2006.07.014)
  18. Gnanadhas DP, Ben Thomas M, Elango M, Raichur AM, Chakravorty D. Chitosan-dextran sulphate nanocapsule drug delivery system as an effective therapeutic against intraphagosomal pathogen Salmonella. *Journal of Antimicrobial Chemotherapy*. 2013;68(11):2576–1286. Available from: [doi.org/10.1093/jac/dkt252](https://doi.org/10.1093/jac/dkt252)
  19. Le-Tien C, Millette M, Mateescu M-A, Lacroix M. Modified alginate and chitosan for lactic acid bacteria immobilization. *Biotechnology and applied biochemistry*. 2004;39:347–354. Available from: [doi.org/10.1042/BA200301588](https://doi.org/10.1042/BA200301588)
  20. Xie S, Yang F, Tao Y, Chen D, Qu W, Huang L. Enhanced intracellular delivery and antibacterial efficacy of enrofloxacin-loaded docosanoic acid solid lipid nanoparticles against intracellular Salmonella. *Scientific Reports*. 2017;7:1–9. Available from: <http://dx.doi.org/10.1038/srep41104>
  21. Zheng Y, Ou Y, Zhang Y, Zheng B, Zeng S, Zeng H. Effects of pullulanase pretreatment on the structural properties and digestibility of lotus seed starch-glycerin monostearin complexes. *Carbohydrate Polymers journal*. 2020;240:116324. Available from: [doi.org/10.1016/j.carbpol.2020.116324](https://doi.org/10.1016/j.carbpol.2020.116324)
  22. Alarifi S, Massadeh S, Al-Agamy M, Al Aamery M, Al Bekairy A, Yassin AE. Enhancement of ciprofloxacin activity by incorporating it in solid lipid nanoparticles. *Tropical Journal of Pharmaceutical Research*. 2020;19(5):909–918. Available from: [doi.org/10.4314/tjpr.v19i5.1](https://doi.org/10.4314/tjpr.v19i5.1)
  23. Mao S, Shuai X, Unger F, Simon M, Bi D, Kissel T. The depolymerization of chitosan: Effects on physicochemical and biological properties. *International Journal of Pharmaceutics*. 2004;281(1–2):45–54. Available from: [doi.org/10.1016/j.ijpharm.2004.05.019](https://doi.org/10.1016/j.ijpharm.2004.05.019)
  24. Talele P, Sahu S, Mishra AK. Physicochemical characterization of solid lipid nanoparticles comprised of glycerol monostearate and bile salts. *Colloids Surfaces B Biointerfaces*. 2018;172:517–525. Available from: [doi.org/10.1016/j.colsurfb.2018.08.067](https://doi.org/10.1016/j.colsurfb.2018.08.067)
  25. Ali SW, Rajendran S, Joshi M. Synthesis and characterization of chitosan and silver loaded chitosan nanoparticles for bioactive polyester. *Carbohydrate Polymers*. 2011;83(2):438–446. Available from: [doi.org/10.1016/j.carbpol.2010.08.004](https://doi.org/10.1016/j.carbpol.2010.08.004)
  26. Carrillo-Navas H, Pérez-Alonso C, Fouconnier B, Vernon-Carter EJ, Alvarez-Ramírez J. Inertial effects of adsorbed glycerol monostearate crystals on the shear rheology of water/canola oil interfaces. *Journal of Food Engineering*. 2014;125(1):112–118. Available from: [doi.org/10.1016/j.jfoodeng.2013.10.025](https://doi.org/10.1016/j.jfoodeng.2013.10.025)
  27. Khanna K, Sharma N, Rawat S, Khan N, Karwasra R, Hasan N. Intranasal solid lipid nanoparticles for management of pain: A full factorial design approach, characterization & Gamma Scintigraphy. *Chemistry and Physics of Lipids*. 2021;236:105060. Available from: [doi.org/10.1016/j.chemphyslip.2021.105060](https://doi.org/10.1016/j.chemphyslip.2021.105060)
  28. Ghadge D, Nangare S, Jadhav N. Formulation, optimization, and in vitro evaluation of anastrozole-loaded nanostructured lipid carriers for improved anticancer activity. *Journal of Drug Delivery Science and Technology*. 2022;72:103354. Available from: [doi.org/10.1016/j.jddst.2022.103354](https://doi.org/10.1016/j.jddst.2022.103354)
  29. Journal AI, Yasir M, Vir U, Sara S, Chauhan I, Gaur PK. Solid lipid nanoparticles for nose to brain delivery of donepezil : formulation , optimization by Box – Behnken design , in vitro and in vivo evaluation. *Artificial Cells, Nanomedicine, and Biotechnology*. 2018;46(8):1838–1851. Available from: [doi.org/10.1080/21691401.2017.1394872](https://doi.org/10.1080/21691401.2017.1394872)